Coherent control of the exciton and exciton-biexciton transitions in the generation of nonlinear wave-mixing signals in a semiconductor quantum well

Tobias Voss,* Ilja Rückmann, and Jürgen Gutowski
Institut für Festkörperphysik, Universität Bremen, P.O. Box 330 440, D-28334 Bremen, Germany

Vollrath Martin Axt and Tilmann Kuhn
Institut für Festkörpertheorie, Universität Münster, Wilhelm-Klemm-Strasse 10, D-48149 Münster, Germany
(Received 20 September 2005; revised manuscript received 21 December 2005; published 9 March 2006)

By use of an optical coherent-control technique we demonstrate and analyze the control of transitions involved in the generation of four-wave-mixing signals in a semiconductor quantum well for the two different four-wave-mixing directions and for different sequences of the excitation pulses. Results are presented for frequency- as well as for time-resolved signals. A doubling of the coherent switching frequency is found which occurs if the laser pulses performing the control process contribute quadratically to the wave-mixing signal. A direct comparison between experiment and microscopic theory reveals how the coherent-control process acts on the coherent polarization of the exciton-biexciton system in all different configurations. An additional interpretation of the experimental results based on a simplified few-level model is able to provide an intuitive understanding of the relevant processes which govern the coherent control of the excitonic and biexcitonic wave-mixing polarizations.

DOI: 10.1103/PhysRevB.73.115311 PACS number(s): 78.67.De, 73.21.Fg, 71.35.−y, 78.47.+p

I. INTRODUCTION

In the past decade the coherent dynamics of excitonic excitations in semiconductors has been a field of intense research because of its importance for the understanding of semiconductor laser dynamics[1] as well as for the possibility to investigate fundamental properties of quantum-mechanical many-particle systems such as Coulomb-correlation effects.[2–10] The latter ones manifest themselves especially in nonlinear optical signals, and their coherent dynamics can be investigated by different experimental ultrafast-spectroscopy techniques such as pump-and-probe or wave-mixing spectroscopy.[2,3]

In various experiments the dependence of spectrally resolved wave-mixing signals—i.e., nonlinear signals generated by effects of at least third order in the electric field—on various parameters has been analyzed to distinguish between different processes which contribute to the nonlinear excitonic response of a semiconductor.[6,11–17] The response is strongly governed by many-particle processes like biexciton formation, excitation-induced dephasing, or local-field contributions. These contributions have been analyzed both experimentally and theoretically as a function of the polarization states of the excitation pulses as well as of the polarization state of the nonlinear signal itself, the absolute and relative intensities of the laser pulses, and their spectral positions.[18–28] In this way, even contributions resulting from high-order Coulomb correlations have been shown to play an important role for the creation of the coherent optical response of a semiconductor in spectrally resolved four- and six-wave-mixing experiments and simulations.[3,4,12–14,29–32]

Recently, not only the observation of the coherent dynamics of the optically generated excitonic polarization but also its targeted manipulation on ultrashort time scales has been subject to intense research. Excitonic polarizations, populations, and the spin orientation of the excitons have been shown to be controllable in the coherent regime.[30,32–40] In a similar way, the optical generation and manipulation of charge currents, spin-polarized currents, and pure spin currents without net charge currents have been subject to extensive experimental and theoretical investigations.[41–43] In zero-dimensional semiconductor quantum-dot systems which possess a δ-function-like density of states the coherent manipulation of the optical transitions in the exciton-biexciton system has even been exploited to demonstrate a simple quantum logic gate.[44]

In the present work we focus on excitonic transitions in two-dimensional quantum-well systems which are used to generate a nonlinear polarization—i.e., a nonlinear optical response of the semiconductor to an exciting laser field. Our work directly demonstrates the coherent control of the relevant optical transitions of the exciton-biexciton system in a quantum well during the generation of a nonlinear four-wave-mixing signal. This is achieved experimentally by use of a coherent-control technique which utilizes a pair of collinearly propagating phase-locked laser pulses which excite the sample exclusively at the heavy-hole exciton and exciton-biexciton resonances. The experimental results are in good agreement with simulations based on a fully microscopic theory which accounts for all optical effects up to third order in the electric field.[45,46] A qualitative understanding for all essential dependences of the signals can be obtained from a phenomenological model based on a simplified few-level system. The results provide insight into the nature of the elementary processes which govern the coherent manipulation of the nonlinear excitonic polarization on ultrashort time scales. Compared to our previous work[47,48] we observe and analyze the signals not only with respect to a phase shift. Since we use a wide-band-gap quantum-well sample with a sharper exciton resonance than in previous

experiments and extremely low excitation densities, we are able to present qualitatively features in the coherent-control signal. In particular, we find a doubled switching frequency of the signal for the four-wave-mixing direction $2k_1$-k_2. In our previous experiments both the higher excitation densities[47] and the much larger inhomogeneous broadening of the exciton resonance[48] had obscured this important feature. Additionally, we are now able to present real-time-resolved measurements of the coherent wave-mixing polarization which not only complement our spectrally resolved measurements but provide additional insight into the way of action of the coherent control in the exciton-biexciton system. In particular, these investigations allow for a precise analysis of the relative phases of the coherent polarizations after the coherent-control process. For the limiting case of ultrafast coherent dynamics at low excitation densities, which is realized in all our present experiments, a complete microscopic theory is available within the density matrix formalism via the use of the method of dynamics controlled truncation.[45,46] This allows us to perform a conclusive quantitative comparison of our experiments with the theory which provides additional information about the coherent-control process. The combined experimental and theoretical treatment enables us, e.g., to unambiguously identify the precise switching frequency of the signals at the ground-state–to–exciton and exciton–to–biexciton transitions. All results taken together provide a detailed picture of the action of the coherent control in the exciton-biexciton system in semiconductor quantum wells which may find its application in the targeted manipulation of semiconductor systems in quantum optics.

II. EXPERIMENTAL SETUP

The time-integrated, spectrally resolved degenerate transient four-wave-mixing (FWM) experiments were carried out on a 10-nm ZnSe single quantum well which is embedded within ZnSSe cladding layers and was pseudomorphically grown by molecular-beam epitaxy on a (001) GaAs substrate. For the experiments which were performed in transmission geometry at a temperature $T=4$ K the substrate had been carefully removed by wet chemical etching. The heavy-hole exciton resonance is separated from the free-electron–hole continuum by a binding energy of $\sim$20 meV. For the ground-state–to–exciton transition (GET) we find a transition energy of $E_{\mathrm{GET}}=2.813$ eV. From linear transmission as well as wave-mixing spectroscopy a linewidth of $\sim$0.8 meV was deduced.

A sketch of the setup of the coherent-control experiment is shown in Fig. 1. A phase-locked pulse pair with an internal time distance t_{int} is generated by use of an actively stabilized Michelson interferometer with a temporal resolution of 40 attoseconds and hits the sample from a direction k_1. In the following, the basic temporal separation of the pulses on a femtosecond time scale will be denoted by t_{int}^0 whereas the fine-tuning on an as time scale will be referred to as Δt_{int}—i.e., $t_{\mathrm{int}}=t_{\mathrm{int}}^0+\Delta t_{\mathrm{int}}$.

An additional single pulse incident from a different direction k_2 is delayed by a time t_{del} with respect to the first pulse

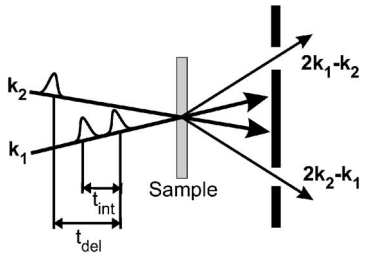

FIG. 1. Experimental setup for the coherent control experiments. The FWM signal is recorded in both directions $2k_2$-k_1 (first order of diffraction of the single pulse) and $2k_1$-k_2 (first order of diffraction of the pulse pair) which are not equivalent.

of the pulse pair with a mechanical delay line (see Fig. 1). The interplay of the polarizations induced by the k_1 and k_2 pulses leads to diffracted signals. We have recorded FWM signals in both directions $2k_2$-k_1 and $2k_1$-k_2, respectively. In a simple picture the first direction corresponds to the first order of diffraction of the single pulse, the second to the first order of diffraction of the pulse pair. For both directions t_{del} will be positive if the single k_2 pulse arrives at the sample last.[49] By use of Pockels cells in each laser beam path the polarization states of the k_1 and k_2 pulses are set to a cross-linear (xy) configuration.

All laser pulses have the same intensity and are generated by a frequency-doubled, self-mode-locked titanium-sapphire laser which produces nearly transform-limited pulses with a temporal width of 120 fs (full width at half maximum). The spectral position of the pulses is chosen such that the spectrum covers both the exciton and exciton-biexciton transitions. The FWM signal is spectrally resolved by a grating spectrometer with a resolution of $\Delta\lambda=0.03$ nm ($\Delta E=0.2$ meV at $E=2.81$ eV) and finally recorded with a liquid-nitrogen-cooled charge-coupled-device (CCD) camera. Additionally, real-time-resolved measurements of the transients of the FWM signal were performed by use of an up-conversion technique. The sum-frequency generation of the signal and an infrared reference pulse (wavelength 880 nm, temporal width $\sim$80 fs) in a BBO crystal was used to perform a cross-correlation measurement as a function of the delay between the signal and reference pulse t_{upc}. In this case the measured signal corresponds to a convolution between the signal and reference pulse which gives the real-time-resolved transients of the signal in a good approximation on time scales much larger than 80 fs (temporal width of the infrared pulse). It was found in the experiments that by use of the up-conversion technique t_{int}^0 could be adjusted with an accuracy of 25 fs.

The excitonic transitions which are involved in the generation of the wave-mixing signal can be visualized by considering the schematic energy diagram for the exciton-biexciton system in Fig. 2. Starting from the unexcited ground state of the semiconductor an excitonic polarization can be created by the absorption of a photon at the energy position of the exciton transition. In general, an excitation with left or right circularly polarized photons leads to two degenerate exciton states with opposite spin orientations. Starting from the excitonic states the absorption of a second

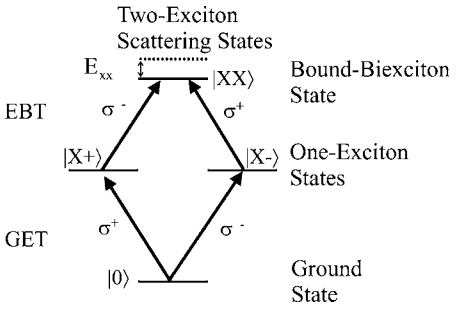

FIG. 2. Schematic energy diagram of the exciton-biexciton system.

photon with a spin being opposite to that of the first one can lead to the excitation of the bound-biexciton state. Consequently, the energy corresponding to this second transition [exciton-biexciton transistion (EBT)] is $E_{\mathrm{EBT}}=E_{\mathrm{GET}}-E_{\mathrm{B}}$ and therefore less than the photon energy corresponding to the GET (E_{B} denotes the biexciton binding energy and amounts to=4.8 meV for the sample used in this work). Since for all experiments and simulations discussed here the excitation pulses in directions k_1 and k_2 are cross-linearly polarized, the signal at the GET is strongly reduced and its strength is just comparable to that at the EBT,[19,27,50] which is favorable for the investigation of the simultaneous coherent control of the GET and EBT.

III. MICROSCOPIC THEORY

The FWM experiments with coherent control of the GET and EBT were simulated by use of a fully microscopic theory. The theory is formulated using the density-matrix approach based on the dynamics-controlled truncation (DCT) scheme.[45,46] We shall consider the so-called coherent limit of the theory which applies when incoherent parts of the dynamics such as, e.g., couplings to a phonon bath can be disregarded.[51,52] On this level of the theory one has to follow the time evolution of two types of dynamical variables: the single-pair transition amplitude Y and the correlated two-pair transition amplitude $\bar{B}$. In terms of expectation values of Fermi operators $\hat{c}_j$ ($\hat{d}_j$) for the annihilation of an electron (hole) in the Wannier state at site j in the conduction (valence) band σ_{c_j} (σ_{v_j}) these variables can be defined as

$$Y_2^1 \equiv \left\langle \hat{Y}_2^1 \right\rangle \equiv \left\langle \hat{d}_1 \hat{c}_2 \right\rangle, \tag{1}$$

$$\bar{B}_{24}^{13} \equiv \left\langle \hat{Y}_2^1 \hat{Y}_4^3 \right\rangle - Y_2^1 Y_4^3 + Y_4^1 Y_2^3. \tag{2}$$

The coupled DCT equations for Y and $\bar{B}$ describe the coherent dynamics exactly up to third order in the laser fields.[45,46,52] In particular, it is worthwhile to note that the Coulomb interaction is treated nonperturbatively which is crucial not only for the occurrence of the Coulomb-related discrete exciton and biexciton resonances but also for the Coulomb-correlated continuum where the standard perturbation treatment in terms of the second-order Born approximation is known to lead to artificial divergences.[53,54] The DCT approach overcomes these divergence problems and allows one to calculate the relative weights of excitonic and biexcitonic contributions to nonlinear signals without adjustable parameters. To be specific, we have used for our numerical implementation the memory kernel formulation described in detail in Ref. 55. For the present paper, we have used a kernel that has been calculated for a two-dimensional quantum well with infinite barrier confinement. The kernel has been determined within a truncated basis set where all states on the 1s-exciton parabola are taken into account. This truncation of the basis set has been extensively tested in Ref. 15 and found to be a reliable approximation under the conditions considered here. The reliability of our level of theory is further confirmed by its success in describing many different signals in excellent agreement with corresponding measurements.[9,27,53–58] In addition, we have checked numerically that the six-particle correlations which have been crucial for certain features of wave-mixing experiments[3,4,12,30,32] are of minor importance for the present excitation conditions and can therefore be disregarded. The resulting nonlinear equations of motion have been solved numerically for the excitation conditions used in the measurements. In principle, the calculated solution implicitly contains repeated interactions with the laser fields up to infinite order. However, in our experiments we have kept the intensities so low that no deviations from the $\chi^{(3)}$ limit were detectable. Consequently, we have performed the calculations with low-pulse areas in order to match the experimental conditions. Also in accordance with the experimental conditions we have accounted for an inhomogeneous broadening of 0.7 meV by sampling over a Gaussian ensemble of gap energies with correlated shifts of single- and two-pair energies. However, it turned out that, apart from slight quantitative improvements of the agreement with the measurements, the inhomogeneous broadening had no noticeable effect on the qualitative behavior discussed below, which is not too surprising considering that the broadening is still moderate.

IV. RESULTS AND DISCUSSION

For the analysis of the coherent control of the nonlinear excitonic polarization different but fixed values of t_{del} and t_{int}^0 were chosen, and the wave-mixing signal was recorded and simulated as a function of the fine-tuning Δt_{int} over a period of 3 fs. For linear excitonic polarizations this procedure should result in a continuous change between constructive and destructive interference which should make the corresponding optical signal oscillate like a cosine function. The questions to be answered in this section are now, how does the nonlinear excitonic polarization behave in this case, and how does the coherent-control scheme affect the signal created by the bound-biexciton state?

The experiments and simulations shown in this paper were performed with $t_{\mathrm{int}}^0=T_{\mathrm{beat}}/2$, where $T_{\mathrm{beat}}=h/E_{\mathrm{B}}$ is the beating period of the coherently excited exciton-biexciton system. From our measurements we determine a value of $T_{\mathrm{beat}}/2=0.425$ ps. The choice of this special value of t_{int}^0 is motivated by the following consideration. If we consider two arbitrary and *independent* transitions having the same energy

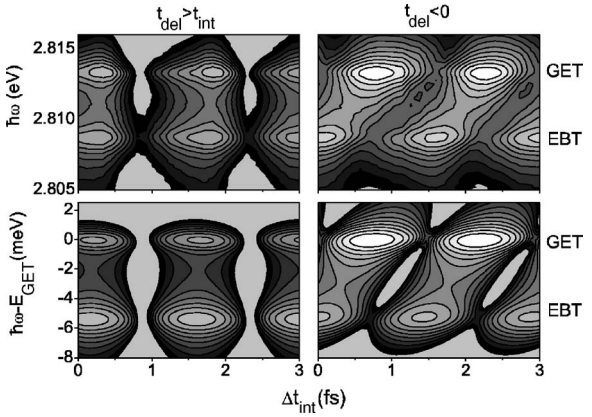

FIG. 3. Spectrally resolved FWM signals with coherent switching detected in direction $2k_2$-k_1. The signals are shown as a function of Δt_{int} for $t_{\mathrm{int}}^0 = T_{\mathrm{beat}}/2$. Top row: experimental results. Bottom row: microscopic simulation. Left (right) column: single k_2 pulse arrives at the sample after (before) the pulse pair. The FWM intensity is shown in contour plots with the gray scale covering two orders of magnitude on a logarithmic scale. GET (EBT): spectral position of exciton (exciton-biexciton) transition.

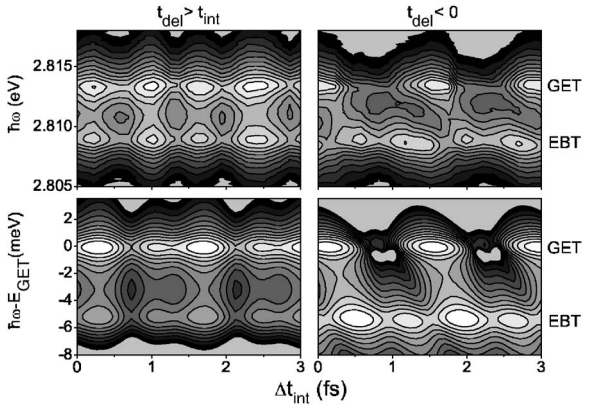

FIG. 4. Spectrally resolved FWM signals (logarithmic scale) with coherent switching detected in direction $2k_1$-k_2. Top row: experimental results. Bottom row: microscopic simulation. Left (right) column: single k_2 pulse arrives at the sample after (before) the pulse pair. $t_{\mathrm{int}}^0 = T_{\mathrm{beat}}/2$.

separation E_{B} as the exciton-biexciton system—i.e., the resonance frequencies being separated by $\Delta\omega = E_{\mathrm{B}}/\hbar$—then $T_{\mathrm{beat}}/2$ would correspond to a time delay at which the two respective coherent polarizations would oscillate with a phase difference of π. Consequently, destructive interference for one of the two polarizations would simultaneously imply constructive interference for the other one if the coherent-control scheme with two phase-locked pulses were applied to the system of independent transitions. This would result in a phase shift of π between the spectrally resolved coherent-control signals being recorded as a function of Δt_{int}. In the following, it will be analyzed to what extent the control of the two correlated transitions GET and EBT exhibits similarities or differences compared to the case of the control of independent transitions.

Since in our setup the wave-mixing polarization is excited by the interplay of three laser pulses (the pulse pair in direction k_1 and the single pulse in direction k_2), we have to distinguish four cases for the creation of the polarization and its coherent control: the single k_2 pulse can arrive at the sample before or after the pulse pair, and in both cases wave-mixing signals are generated and can be measured for the two different directions $2k_2$-k_1 and $2k_1$-k_2. The case where the single pulse arrives between the pulses of the phase-locked pair does not result in a principally different behavior which has been shown before.[48]

The experimental results for all four configurations are shown in Figs. 3 and 4 (top rows) together with the results of the microscopic simulations (bottom rows). In Fig. 3 the signals for the FWM direction $2k_2$-k_1 are depicted in which the phase-locked pulse pair contributes linearly. Figure 4 shows the corresponding results for the FWM direction $2k_1$-k_2 in which the pulse pair contributes quadratically to the signal. The left columns in both figures represent the situations in which the single pulse hits the sample after the pulse pair. Those cases in which the single pulse hits the sample before the pulse pair are shown in the right columns.

A. Results for the FWM direction $2k_2$-k_1

We will first concentrate on the results presented in Fig. 3 for the FWM direction $2k_2$-k_1. The right-hand-side results have been obtained for a value $t_{\mathrm{del}} = -0.1$ ps ($t_{\mathrm{del}} < 0$—i.e., single pulse first). The data of the left column were obtained for $t_{\mathrm{del}} = +1.0$ ps $> t_{\mathrm{int}}$ (single pulse last). Additional experiments and simulations performed for other values of t_{del} (not shown here) clearly confirm that the signatures of the coherent-control traces do not change as long as the principal relationship $t_{\mathrm{del}} > t_{\mathrm{int}}$ or $t_{\mathrm{del}} < 0$ is kept, respectively. The intensities of the spectrally resolved FWM signals are shown in the contour plots over two orders of magnitude encoded in a grey scale where white corresponds to maximum intensity. Their cosinelike oscillations as a function of Δt_{int} exhibit a period of about 1.5 fs corresponding to that expected for a polarization with an energy $E \approx 2.813$ eV. As is evident from Fig. 3, adjusting t_{int}^0 to $t_{\mathrm{int}}^0 = T_{\mathrm{beat}}/2$ results in FWM signals at the GET and EBT which show their maxima and minima *simultaneously* if $t_{\mathrm{del}} > t_{\mathrm{int}}$ but exhibit a relative phase shift of $\Delta\phi = \pi$ if $t_{\mathrm{del}} < 0$. Experiment and microscopic theory are in excellent agreement. A further analysis reveals that the signal at the GET shifts by half a period if t_{del} is changed from $t_{\mathrm{del}} > t_{\mathrm{int}}$ to $t_{\mathrm{del}} < 0$ whereas the minima and maxima of the signal at the EBT stay fixed (compare left and right columns of Fig. 3). Additionally, in the left column both signals oscillate with the frequency corresponding to the GET while in the right column the signal at the GET oscillates with the frequency corresponding to the EBT and the signal at the EBT oscillates with the frequency corresponding to the GET. This can be unambiguously shown by inspecting the values of Δt_{int} for which the theory curves exhibit minimum intensity.

It has been pointed out many times by different authors that a quantitative simulation of FWM signals emitted after resonant excitation at the exciton energy requires a microscopic description which accounts for correlated two-pair continua.[7–10,27,53–58] Indeed, the excellent agreement between our microscopic theory and the measurements confirms once again that this level of theory is capable of capturing all

essential features of such experiments. In this way our calculations also give firm evidence that the observed features are mainly caused by coherent third-order ($\chi^{(3)}$) processes in the quantum well. However, it can be hard to develop an intuitive understanding of the pertinent physics based on a purely numerical solution. To bridge this gap it turns out to be instructive to consider a phenomenological few-level model for the qualitative interpretation of the measurements in addition to the microscopic analysis. When applied to the exciton-biexciton system many aspects of the corresponding nonlinear dynamics have been successfully addressed by using few level models similar to the level scheme shown in Fig. 2 (cf. Refs. 5, 18, 20, and 59–61). The formal relation between the microscopic theory and few-level approaches has been established in Ref. 62, providing a further justification for the latter within certain limits. Indeed, with those features which do not crucially depend on the presence of the continua it is often even possible to obtain good quantitative fits of corresponding measurements,[5,18,20,59–61] especially when the few-level description is extended by further phenomenological additives such as a local field parameter.[20,59,61] Here, we are not looking for a good quantitative fit; instead, we are looking for the most simple level of theory which still describes the most striking qualitative features of our experiments. In order to obtain compact analytical results we shall concentrate for the present discussion on a fixed linear excitation. This allows us to further reduce the level scheme from Fig. 2 and to consider a model with only three discrete states: the ground state $\langle 0 \rangle$, the single-exciton state $|X\rangle$, which is reached by the linear excitation, and the biexciton state $|B\rangle$. We shall denote the off-diagonal density matrix elements that represent the GET and EBT signal contributions by $Y_{\mathrm{GET}} \equiv \langle |0\rangle\langle X| \rangle$ and $Y_{\mathrm{EBT}} \equiv \langle |X\rangle\langle B| \rangle$, respectively. The corresponding FWM signals measured in direction $2k_\ell$-k_j are proportional to the Fourier components $Y_{\mathrm{GET}}^{2k_\ell - k_j}$ and $Y_{\mathrm{EBT}}^{2k_\ell - k_j}$ where $2k_\ell$-k_j can be either $2k_2$-k_1 or $2k_1$-k_2. These transition densities obey to leading order in the laser field the following equations of motion which have been derived disregarding any dephasing in order to keep the discussion simple:

$$\left(i\frac{\partial}{\partial t} - \omega_{\mathrm{GET}}\right) Y_{\mathrm{GET}}^{2k_\ell - k_j} = \mu_{\mathrm{GET}} E^{k_\ell} 2 Y_{\mathrm{GET}}^{k_\ell} Y_{\mathrm{GET}}^{k_j *} - \mu_{\mathrm{EBT}} E^{k_j *} B^{2k_\ell} + \mathcal{O}(E^5), \tag{3}$$

$$\left(i\frac{\partial}{\partial t} - \omega_{\mathrm{EBT}}\right) Y_{\mathrm{EBT}}^{2k_\ell - k_j} = -\mu_{\mathrm{EBT}} E^{k_\ell} Y_{\mathrm{GET}}^{k_\ell} Y_{\mathrm{GET}}^{k_j *} + \mu_{\mathrm{GET}} E^{k_j *} B^{2k_\ell} + \mathcal{O}(E^5), \tag{4}$$

where μ_{GET} and μ_{EBT} describe the dipole coupling (assumed to be real) for the exciton and exciton–to–biexciton transitions and ω_{GET} and ω_{EBT} are the corresponding transition frequencies. $Y_{\mathrm{GET}}^{k_\ell}$ and $Y_{\mathrm{GET}}^{k_j}$ describe the linear response to the laser excitations E^{k_ℓ} and E^{k_j} in k_ℓ or k_j direction. Finally, B^{2k_ℓ} is the $2k_\ell$-Fourier component of the two-photon coherence (TPC) $B \equiv \langle |0\rangle\langle B| \rangle$.

Both the GET and EBT are driven by two types of source terms: the first ($\sim E^{k_\ell} Y_{\mathrm{GET}}^{k_\ell} Y_{\mathrm{GET}}^{k_j *}$) represents the Pauli blocking while the second ($\sim E^{k_j *} B^{2k_\ell}$) involves the excitation of the biexcitonic TPC B^{2k_ℓ}. Recalling that $Y_{\mathrm{GET}}^{k_j}$ (B^{2k_ℓ}) is zero before the arrival of a pulse in k_j (k_ℓ) direction it follows immediately from Eqs. (3) and (4) that the Pauli blocking (TPC) term does not contribute to the third-order signal when the k_ℓ (k_j) excitation is completed before any pulse from the other direction strikes the sample. Thus, for a given direction and time ordering ($t_{\mathrm{del}} > t_{\mathrm{int}}$ or $t_{\mathrm{del}} < 0$) there is only a single contribution to each of the transition densities $Y_{\mathrm{GET}}^{2k_\ell - k_j}$ and $Y_{\mathrm{EBT}}^{2k_\ell - k_j}$. Of course, this feature of the phenomenological model makes the discussion particularly transparent, but it should be kept in mind that microscopic models do not share this property because mean-field contributions and two-pair correlations add to the signals for both time orderings.

1. Pulse sequence: Single pulse last

It is straightforward to solve Eqs. (3) and (4) analytically for the case of ultrafast (δ-pulse) excitation.[63] Let us first discuss the signal in $2k_2$-k_1 direction for the configuration $t_{\mathrm{del}} > t_{\mathrm{int}}$ (single pulse last), where only the Pauli blocking nonlinearity contributes. We find

$$Y_{\mathrm{GET}}^{2k_2 - k_1} = A_{\mathrm{GET}}(t, t_{\mathrm{del}})(1 + \mathrm{e}^{-i\omega_{\mathrm{GET}} t_{\mathrm{int}}}), \tag{5}$$

$$Y_{\mathrm{EBT}}^{2k_2 - k_1} = A_{\mathrm{EBT}}(t, t_{\mathrm{del}})(1 + \mathrm{e}^{-i\omega_{\mathrm{GET}} t_{\mathrm{int}}}), \tag{6}$$

where A_{GET} and A_{EBT} are complex amplitudes that depend only on the real time t and the delay t_{del}. Their explicit form is unimportant for the following discussion of the dependences on the control delay time t_{int} and therefore not given. The control delay t_{int} enters the expression for both GET and EBT in the same way via the factor $(1+\mathrm{e}^{-i\omega_{\mathrm{GET}} t_{\mathrm{int}}})$ which, depending on the value of t_{int}, results either in constructive or destructive interference. Physically, this can be understood by noting that for this configuration each of the phase locked k_1 pulses in a first step creates a contribution to the linear transition amplitude $Y_{\mathrm{GET}}^{k_1}$. Then, in a second step the k_2 pulse generates the FWM signal in the $2k_2$-k_1 direction which essentially tests the value of $Y_{\mathrm{GET}}^{k_1}$ after the second pulse. The factor $(1+\mathrm{e}^{-i\omega_{\mathrm{GET}} t_{\mathrm{int}}})$ simply reflects the phase difference accumulated by the free oscillation of $Y_{\mathrm{GET}}^{k_1}$ between the first and second k_1 pulses. Since the pulse pair contributes linearly in this FWM direction, destructive interference for the GET will result in no FWM signal at all because the quantum-well system will be in the unexcited ground state after the two phase-locked pulses have reached the sample. If, on the other hand, the pulse pair is adjusted for constructive interference at the GET, the interplay with the polarization induced by the k_2 pulse (this pulse always induces contributions at the GET and EBT since its spectrum always covers both resonances) will create a FWM signal at the energy positions of both the GET and EBT. Thus, in this configuration the control of the FWM signal results from the interference of the linear polarizations $Y_{\mathrm{GET}}^{k_1}$ created in the first step by the two control pulses. This also explains why both transitions (GET and EBT) change with varying t_{int} si-

multaneously from destructive to constructive interference, both with the same frequency ω_{GET}. This is exactly the behavior observed in our measurements as well as in the numerical solution of the microscopic model (cf. left panels of Fig. 3).

2. Pulse sequence: Single pulse first

For the configuration $t_{\mathrm{del}}<0$ where the k_2 pulse hits the sample first, a $2k_2$-k_1 FWM signal can be generated only if the single pulse induces a TPC. Only in this way can two k_2 photons be stored in the quantum-well system until the arrival of the phase-locked pulse pair. The corresponding GET and EBT FWM signals are then, according to Eqs. (3) and (4), generated by the TPC nonlinearities $\sim E^{k_1*}B^{2k_2}$. The temporal behavior of the TPC sources in the ultrafast pulse limit consists of two short impulses because of the factor E^{k_1*}. Thus, each of the two control pulses creates a GET and an EBT FWM signal which then oscillate with the respective frequencies ω_{GET} and ω_{EBT}. In contrast to the case $t_{\mathrm{del}}>t_{\mathrm{int}}$ the control of the $2k_2$-k_1 FWM signal for $t_{\mathrm{del}}<0$ results from the constructive or destructive interference of the third-order polarizations that are created by the two control pulses. This has important consequences. For example, the GET FWM signal oscillates in real time with the frequency ω_{GET}. Consequently, the phase of the FWM signal generated by the first k_1 pulse will change due to the oscillation until the arrival of the second k_1 pulse by an amount of $\delta\varphi=\omega_{\mathrm{GET}}t_{\mathrm{int}}$. In a linear interference experiment such as realized for the linear polarizations $Y^{k_1}_{\mathrm{GET}}$ discussed above, the phase $\delta\varphi$ accumulated by the oscillation of the first transition would completely determine the phase difference between the two transitions that are brought to an interference. Thus, the period for one cycle from constructive via destructive and back to constructive interference would be given by the oscillation period $2\pi/\omega_{\mathrm{GET}}$. In contrast to this, the FWM transitions are generated in a nonlinear process. Due to the coupling $\sim E^{k_1*}B^{2k_2}$, the initial value of an FWM signal generated by a given k_1 pulse is proportional to the value of the TPC B^{2k_2} at the arrival time of the pulse. Thus, the oscillation of B^{2k_2} with frequency $\omega_{\mathrm{TPC}}=\omega_{\mathrm{GET}}+\omega_{\mathrm{EBT}}$ leads to an additional phase difference of $-\omega_{\mathrm{TPC}}t_{\mathrm{int}}$ between the initial values of the FWM polarizations that are generated by the two k_1 pulses. This is reflected by the analytical solution of Eq. (3). Indeed, the t_{int} dependence of the GET for times $t>t_{\mathrm{int}}$ turns out to be

$$Y^{2k_2-k_1}_{\mathrm{GET}} \propto (1+\mathrm{e}^{-i\omega_{\mathrm{EBT}}t_{\mathrm{int}}}) \quad \text{for } t>t_{\mathrm{int}}, t_{\mathrm{del}}<0. \tag{7}$$

The analogous analysis for the EBT yields

$$Y^{2k_2-k_1}_{\mathrm{EBT}} \propto (1+\mathrm{e}^{-i\omega_{\mathrm{GET}}t_{\mathrm{int}}}) \quad \text{for } t>t_{\mathrm{int}}, t_{\mathrm{del}}<0. \tag{8}$$

Thus, the simplified phenomenological model explains why in the microscopic calculations for this configuration the FWM signal at the GET is modulated with a frequency corresponding to the EBT and vice versa. Moreover, for $t_{\mathrm{int}}=T_{\mathrm{beat}}/2$ this difference of the modulation frequencies enables a separate switching of the FWM signals at the GET and EBT with a phase difference of $\Delta\varphi=\pi$ as experimentally demonstrated in the right column of Fig. 3 in accordance with the corresponding microscopic simulation.

B. Results for the FWM direction $2k_1$-k_2

For the other FWM direction $2k_1$-k_2 a completely different behavior of the coherent-control signals is found (see Fig. 4). This is of course expected since now the pulse pair which is responsible for the coherent control of the transitions enters quadratically in the generation of the FWM signal; i.e., two photons from the pulse pair together with an additional photon from the single k_2 pulse are used to create a signal photon. For the results shown in the left column (single pulse last) the delay was set to $t_{\mathrm{del}}=+0.7$ ps; in the right column the experiment and simulations were performed with $t_{\mathrm{del}}=-0.1$ ps (single pulse first).

1. Pulse sequence: Single pulse last

Again, if the single pulse hits the sample last, no phase shift between the signals at the two resonances is found; i.e., the FWM signals at the GET and EBT are switched on and off simultaneously (left column, $t_{\mathrm{del}}>t_{\mathrm{int}}$). Note that this behavior is qualitatively identical to the same sequence of the excitation pulses for the other FWM direction (compare left columns of Figs. 3 and 4). However, now a doubling of the switching frequency as a function of Δt_{int} compared to the results for the FWM direction $2k_2$-k_1 occurs at the spectral positions of both the GET and EBT. A related phenomenon is known from atomic physics where control time dependences were found which did comprise a frequency doubled component when two-photon transitions are directly coherently manipulated by use of a phase-locked pulse pair.[64]

In order to interpret these results with our phenomenological three-level model we first note that according to Eqs. (3) and (4) the signal in the $2k_1$-k_2 direction for $t_{\mathrm{del}}>t_{\mathrm{int}}$ results only from the TPC nonlinearity which implies that the pulse pair now excites the TPC B^{2k_1} and then the FWM signals are later generated when the k_2 pulse arrives. Thus, this time the controlled FWM signals actually reflect the control of the TPC. The control of a TPC is, however, qualitatively different from the control of a single-photon coherence. In the latter case the controlled signal is the linear superposition of the signals that would be obtained separately from each of the two pulses. Of course, also each of the two pulses of the pair alone would create a TPC, but nevertheless the controlled TPC signal does not equal the sum of these two TPC contributions. Instead, there is an additional pathway that needs to be taken into account. This is most easily seen by looking at the equation of motion for B^{2k_1} which reads

$$\left(i\frac{\partial}{\partial t}-\omega_{\mathrm{TPC}}\right)B^{2k_1}=-\mu_{\mathrm{EBT}}E^{k_1}Y^{k_1}_{\mathrm{GET}}+\mathcal{O}(E^4). \tag{9}$$

According to Eq. (9) the TPC is driven by sources proportional to $E^{k_1}Y^{k_1}_{\mathrm{GET}}$. Thus, in addition to the sources formed by one of the pulses and the linear polarization $Y^{k_1}_{\mathrm{GET}}$ generated by the same pulse there is a further contribution to B^{2k_1} driven by a source where the second k_1 pulse interacts with the polarization created by the first one. Again, it is easy to derive explicit expressions for the resulting GET and EBT FWM signals. The fact that the control of both FWM signals is governed by the control of B^{2k_1} is reflected by identical t_{int}

dependences of the GET and EBT. Thus, the three-level model explains the observed simultaneous switching of these signals. A closer look reveals that both FWM polarizations are proportional to the control factor

$$F(t_{\mathrm{int}}) = \frac{1}{2} + \frac{1}{2}e^{i\omega_{\mathrm{TPC}}t_{\mathrm{int}}} + e^{i\omega_{\mathrm{EBT}}t_{\mathrm{int}}}. \tag{10}$$

This factor contains a term that oscillates with frequency $\omega_{\mathrm{TPC}}=\omega_{\mathrm{GET}}+\omega_{\mathrm{EBT}}$ which is about twice the value of either ω_{GET} or ω_{EBT}. For $t_{\mathrm{int}}\approx T_{\mathrm{beat}}/2$ we have $e^{i\omega_{\mathrm{EBT}}t_{\mathrm{int}}}\approx -e^{i\omega_{\mathrm{GET}}t_{\mathrm{int}}}$ and therefore the control factor can be combined to

$$F(t_{\mathrm{int}}) \overset{t_{\mathrm{int}}\approx T_{\mathrm{beat}}/2}{\rightarrow} 1 - \frac{1}{2}(1 + e^{i\omega_{\mathrm{GET}}t_{\mathrm{int}}})^2. \tag{11}$$

The experiments monitor the intensity emitted in a FWM direction, and thus it is the absolute square of the factor in Eq. (11) which determines the t_{int} dependence in our measurements. Taking the absolute square of Eq. (11) yields

$$|F(t_{\mathrm{int}})|^2 = \frac{3}{2} - \frac{1}{2}\cos(2\omega_{\mathrm{GET}}t_{\mathrm{int}}). \tag{12}$$

This should be compared with the absolute squares of the corresponding factors in Eqs. (7) and (8) which read

$$|1 + e^{-i\omega_{\mathrm{X}}t_{\mathrm{int}}}|^2 = 2[1 + \cos(\omega_{\mathrm{X}}t_{\mathrm{int}})], \tag{13}$$

where ω_{X} is either ω_{EBT} or ω_{GET}. Thus, in agreement with the numerical studies within the microscopic model, our simple model indeed predicts a frequency doubling for the modulation of the control signal as it is observed in our experiments [cf. Fig. 4 (left panels)].

2. Pulse sequence: Single pulse first

The right column of Fig. 4 shows the $2k_1$-k_2 FWM signals for the configuration in which the single pulse arrives at the sample before the pulse pair. As for $t_{\mathrm{del}}<0$ in the $2k_2$-k_1 direction, a phase shift between the signals at the GET and EBT occurs. However, the switching frequency of the signal at the EBT is again doubled whereas the signal at the GET is modulated just with the fundamental frequency (compare with right column of Fig. 3). Also for the configuration $2k_1$-k_2 an overall excellent qualitative agreement between experiment and microscopic simulation can be seen. Applying the three-level model to this case we find the following dependences on the control delay t_{int}:

$$Y_{\mathrm{GET}}^{2k_1-k_2} \propto (1 + e^{i\omega_{\mathrm{GET}}t_{\mathrm{int}}})^2 \quad \text{for } t > t_{\mathrm{int}}, t_{\mathrm{del}} < 0, \tag{14}$$

$$Y_{\mathrm{EBT}}^{2k_1-k_2} \propto F(t_{\mathrm{int}}) \quad \text{for } t > t_{\mathrm{int}}, t_{\mathrm{del}} < 0, \tag{15}$$

where $F(t_{\mathrm{int}})$ is the control factor defined in Eq. (10). In this configuration the control is caused by an interference of the FWM signals produced by the first and second k_1 pulses via the Pauli blocking nonlinearity [i.e., the term $\sim E^{k_1}Y_{\mathrm{GET}}^{k_1}Y_{\mathrm{GET}}^{k_2*}$ in Eqs. (3) and (4)]. Again, the control signal is not the linear superposition of the FWM signals that would have been produced if each of the k_1 pulses acted alone. This can be easily deduced from Eqs. (3) and (4) by noting that the second k_1 pulse of the pair generates two signal contributions resulting from the coupling to the polarizations created by the first and second pulses.

Taking the absolute square of Eq. (14) we find that the corresponding signal intensity is modulated by a factor of $4[1+\cos(\omega_{\mathrm{GET}}t_{\mathrm{int}})]^2$. Even though due to the squaring this factor has a Fourier component oscillating with twice the frequency ω_{GET}, it has its maxima and minima at the same positions as the factor $2[1+\cos(\omega_{\mathrm{GET}}t_{\mathrm{int}})]$ which according to Eq. (13) corresponds to the absolute square of Eq. (7). In this sense the model predicts a modulation of the signal with the fundamental frequency of the GET. It can thus explain why the measurements shown in the right panel of Fig. 4 do not exhibit a frequency doubling even though the pulse pair enters the signals quadratically. The squaring of the factor $(1+e^{i\omega_{\mathrm{GET}}t_{\mathrm{int}}})$ which reflects the nonlinear character of the control affects the shape of the modulation but not the period between subsequent maxima or minima. In the EBT result the occurrence of frequencies different from ω_{GET} motivates why the GET and EBT signals are not in phase. Furthermore, as discussed before, the control factor F which for $t_{\mathrm{int}} \approx T_{\mathrm{beat}}/2$ combines to the result in Eq. (11) explains the observed frequency doubling, which is also well reproduced within the microscopic approach.

C. Real-time-resolved FWM

To get even more insight into the way of action of the coherent control of the exciton-biexciton system we have performed additional experiments and simulations with real-time resolution. In the theory, of course, the complex signal amplitudes in the real-time and frequency domain are connected by a Fourier transformation. However, as the experiments measure only the intensities phase information gets lost which under certain circumstances can be reconstructed from a combination of both measurements.[65,66] Therefore, time and frequency domain measurements contain complementary information.

The present investigations were carried out for both FWM directions. In Fig. 5 we show the results for the direction $2k_2$-k_1 in which the important features are most distinctly visible. The results for the direction $2k_1$-k_2 (not shown here) are quite similar but experimentally less well resolvable due to the doubled switching frequency of the FWM signal in the coherent-control experiments. In Fig. 5 the measured (right column) and simulated (left column) real-time transients of the FWM signal are shown as a function of Δt_{int} for $t_{\mathrm{int}}^0 = T_{\mathrm{beat}}/2$. In order to facilitate the comparison of the qualitative features we have scaled the t_{upc} axis of the theoretical results in Fig. 5 such that the beating period coincides with the experiment. This scaling accounts for a slight difference of the biexciton binding energy in experiment and theory (see the GET and EBT resonances in Figs. 3 and 4) being due to the idealized modeling of the confinement barriers as well as to the restriction of the basis set to the $1s$-exciton states.[67] As a consequence, in the theory the period of the exciton-biexciton beats possesses a value being slightly different from that in the experiment. The Δt_{int} axes of Fig. 5 can be directly compared to the ones of Fig. 3, thus providing a direct comparison between the spectrally and real-time-

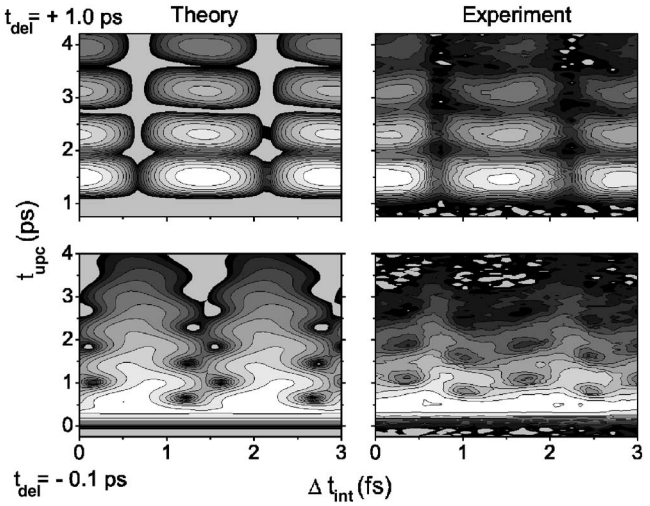

FIG. 5. Coherent control of the FWM signal in the direction $2k_2$-k_1 for $t_{\mathrm{int}}^0 = T_{\mathrm{beat}}/2$. Bottom row: real-time FWM signals (left, simulated; right, measured) as a function of Δt_{int} for $t_{\mathrm{del}} = -0.1$ ps. Top row: same for $t_{\mathrm{del}} = +1.0$ ps. All signals are shown in contour plots on a logarithmic grey scale spanning two orders of magnitude. The Δt_{int} axes are directly comparable with the ones in Fig. 3.

resolved data. The real-time transients can be obtained as vertical cuts along the t_{upc} axis through the contour plots. The top row gives the results for a positive delay (k_2 pulse arrives last), the bottom row for a negative delay (k_2 pulse arrives first). For the first case the spectrally resolved FWM signals at the GET and EBT simultaneously reach their maximum and minimum values as a function of Δt_{int}. The peak intensity of the transients is clearly affected by the coherent-control process; however, the overall shape of the transients stays constant. If a significant signal can be measured, the transients always show a strong beating which is due to the coherent excitation of both the GET and EBT by the ultrashort laser pulses. Additionally, the phase of the exciton-biexciton beats stays constant for all measured values of Δt_{int}. The transients are affected by the coherent control directly after the creation of the coherent FWM polarization—i.e., directly after the arrival of the single k_2 pulse. This supports the explanation that for this FWM direction and sequence of the excitation pulses (k_2 last) the k_2 pulse essentially tests the linear polarization induced by the interplay of the phase-locked k_1 pulses.

The behavior of the transients changes completely if the sequence of the pulses is reversed such that the single pulse hits the sample first (bottom row). It can be clearly seen that the nonlinear FWM signal starts to build up directly after the arrival of the first k_1 pulse at $t_{\mathrm{upc}} = 0$ but does not show a variation as a function of Δt_{int} until the second pulse of the pair arrives at $t_{\mathrm{int}}^0 = T_{\mathrm{beat}}/2$. Only for $t_{\mathrm{upc}} > t_{\mathrm{int}}^0$ a coherent manipulation of the nonlinear FWM signal can be clearly observed which supports the interpretation of this process as a *coherent control of the FWM polarization*.

In contrast to the results presented in the top row of Fig. 5 the signal in the bottom row clearly shows a change of both the amplitude and phase of the exciton-biexciton beats superimposed to the transients. This is a clear indication that in this case the GET and EBT are separately addressed by the coherent control. In the spectrally resolved measurements this behavior results in the already mentioned phase shift between the coherent-control signals at the energy positions of the GET and EBT. The real-time transients, however, reveal even more information because the transients at intermediate positions between constructive or destructive interference for either of the two resonances clearly show a phase shift of $\Delta\varphi = \pi$ of their respective beat structure (compare the position of the black "holes" which occur in the contour plots directly before and after the maximum signal). Due to this phase shift of the beat structure, the transients for these different values of Δt_{int} are not equivalent whereas the respective spectra do not show any qualitative difference. For these values of Δt_{int} the spectra just show comparable FWM intensities at both resonances. This result confirms again the complementarity of real-time and frequency-domain information. The real-time transients provide an independent and direct proof that the GET and EBT can be separately addressed in coherent-control experiments.

V. CONCLUSIONS

In conclusion, we have presented a detailed experimental and theoretical investigation of the optical coherent control of the exciton-biexciton system in a semiconductor quantum well. The coherent manipulation of a nonlinear wave-mixing polarization was analyzed for different sequences of the excitation pulses and for the two different four-wave-mixing directions $2k_1$-k_2 and $2k_2$-k_1 which are not equivalent since, in addition to the single k_2 pulse, a phase-locked pulse pair is applied from direction k_1. Frequency-domain measurements were supplemented by real-time results which give access to complementary information. The experiments were analyzed by simulations based on a microscopic theory and by analytical formulas derived within a phenomenological few-level model for the exciton-biexciton system. Significant differences for the two FWM directions have been found and explained by the fact that the pulse pair enters in different orders into the generation for the FWM polarization for the two directions. The few-level analysis furthermore revealed that the control of the FWM emission at low excitation densities can be brought about by different mechanisms which can be selected by varying the time ordering of the pulses or the direction of the emission. In the $2k_2$-k_1 direction the control signals reflect the interference of linear polarizations when the pulse pair precedes the k_2 pulse. By reversing the time ordering in this direction the control is due to a superposition of FWM amplitudes. In this configuration each k_1 pulse generates an FWM amplitude independent of the other pulse. By measuring in the $2k_1$-k_2 direction we can monitor the direct nonlinear control of the TPC provided the k_2 pulse is the last pulse. Finally, when the k_2 pulse arrives first at the sample we obtain an interference of FWM amplitudes in the direction $2k_1$-k_2. In this case, the FWM amplitude generated by the second control pulse depends on the polarization produced by the first one, revealing the nonlinear character of the control. In experiments performed in the $2k_1$-k_2 direction where the pulse pair enters quadratically we observed a fre-

quency doubling of the control which is well reproduced by the microscopic simulation and qualitatively explained by the analytical results derived from the simplified three-level model. In fact, the microscopic theory is able to model quantitatively all essential features of the experiments. Recalling again that previous studies[7–10,27,53–58] have indicated the importance of correlated two-pair continuum contributions to FWM signals even when the 1*s* exciton is selectively excited, it is remarkable that all pertinent qualitative features of our present coherent control experiments are well reproduced by a phenomenological three-level model where continua as well as mean-field contributions are completely ignored. In our case, the phenomenological model, therefore, yields helpful insights, leading towards the physical understanding of the measurements.

The results provide the basis for a targeted nonlinear optical manipulation of semiconductor quantum-well samples to selectively enhance or suppress contributions of different, even coupled, excitonic resonances within the spectral range of the excitation pulses.

ACKNOWLEDGMENTS

The authors thank W. Faschinger, Würzburg University, for providing the sample. The authors also thank H. G. Breunig for many fruitful discussions.

*Electronic address: tvoss@ifp.uni-bremen.de

[1] W. W. Chow and S. W. Koch, *Semiconductor-Laser Fundamentals* (Springer, Berlin, 1999).
[2] J. Shah, *Ultrafast Spectroscopy of Semiconductors and Semiconductor Nanostructures* (Springer, Berlin, 1996).
[3] V. M. Axt and T. Kuhn, Rep. Prog. Phys. **67**, 433 (2004).
[4] D. S. Chemla and J. Shah, Nature (London) **411**, 549 (2001).
[5] T. F. Albrecht *et al.*, Phys. Rev. B **54**, 4436 (1996).
[6] D. S. Kim, J. Shah, T. C. Damen, W. Schäfer, F. Jahnke, S. Schmitt-Rink, and K. Köhler, Phys. Rev. Lett. **69**, 2725 (1992).
[7] P. Kner, S. Bar-Ad, M. V. Marquezini, D. S. Chemla, and W. Schäfer, Phys. Rev. Lett. **78**, 1319 (1997).
[8] P. Kner, W. Schäfer, R. Lövenich, and D. S. Chemla, Phys. Rev. Lett. **81**, 5386 (1998).
[9] T. Östreich, K. Schönhammer, and L. J. Sham, Phys. Rev. B **58**, 12920 (1998).
[10] C. Sieh *et al.*, Phys. Rev. Lett. **82**, 3112 (1999).
[11] W. Schäfer, D. S. Kim, J. Shah, T. C. Damen, J. E. Cunningham, K. W. Goossen, L. N. Pfeiffer, and K. Köhler, Phys. Rev. B **53**, 16429 (1996).
[12] S. R. Bolton, U. Neukirch, L. J. Sham, D. S. Chemla, and V. M. Axt, Phys. Rev. Lett. **85**, 2002 (2000).
[13] W. Schäfer, R. Lövenich, N. A. Fromer, and D. S. Chemla, Phys. Rev. Lett. **86**, 344 (2001).
[14] W. Langbein, T. Meier, S. W. Koch, and J. M. Hvam, J. Opt. Soc. Am. B **18**, 1318 (2001).
[15] R. Takayama, N. H. Kwong, I. Rumyantsev, M. Kuwata-Gonokami, and R. Binder, Eur. Phys. J. B **25**, 445 (2002).
[16] R. Lövenich, C. W. Lai, D. Hägele, D. S. Chemla, and W. Schäfer, Phys. Rev. B **66**, 045306 (2002).
[17] J. Wühr, V. M. Axt, and T. Kuhn, Phys. Rev. B **70**, 155203 (2004).
[18] K. Bott, O. Heller, D. Bennhardt, S. T. Cundiff, P. Thomas, E. J. Mayer, G. O. Smith, R. Eccleston, J. Kuhl, and K. Ploog, Phys. Rev. B **48**, 17418 (1993).
[19] H. Wang, J. Shah, T. C. Damen, and L. N. Pfeiffer, Solid State Commun. **91**, 869 (1994).
[20] E. J. Mayer *et al.*, Phys. Rev. B **50**, 14730 (1994).
[21] J. A. Bolger, A. E. Paul, and A. L. Smirl, Phys. Rev. B **54**, 11666 (1996).
[22] G. Bartels, A. Stahl, V. M. Axt, B. Haase, U. Neukirch, and J. Gutowski, Phys. Rev. Lett. **81**, 5880 (1998).
[23] B. Haase, U. Neukirch, J. Gutowski, G. Bartels, A. Stahl, J. Nürnberger, and W. Faschinger, Phys. Status Solidi B **206**, 363 (1998).
[24] B. Haase, U. Neukirch, J. Gutowski, G. Bartels, A. Stahl, V. M. Axt, J. Nürnberger, and W. Faschinger, Phys. Rev. B **59**, R7805 (1999).
[25] A. L. Smirl, in *Semiconductor Quantum Optoelectronics*, Proceedings of the 50th Scottish Universities Summer School in Physics, edited by A. Miller, A. Ebrahimzadeh, and D. M. Finlayson (SUSSP, Edinburgh, 1999).
[26] T. Aoki, G. Mohs, Y. P. Svirko, and M. Kuwata-Gonokami, Phys. Rev. B **64**, 045212 (2001).
[27] V. M. Axt, B. Haase, and U. Neukirch, Phys. Rev. Lett. **86**, 4620 (2001).
[28] S. Wachter, M. Maute, H. Kalt, and I. Galbraith, Phys. Rev. B **65**, 205314 (2002).
[29] V. M. Axt, S. R. Bolton, U. Neukirch, L. J. Sham, and D. S. Chemla, Phys. Rev. B **63**, 115303 (2001).
[30] T. Voss, H. G. Breunig, I. Rückmann, J. Gutowski, V. M. Axt, and T. Kuhn, Phys. Rev. B **66**, 155301 (2002).
[31] A. T. Karathanos, I. E. Perakis, N. A. Fromer, and D. S. Chemla, Phys. Rev. B **67**, 035316 (2003).
[32] H. G. Breunig, T. Voss, I. Rückmann, J. Gutowski, V. M. Axt, and T. Kuhn, J. Opt. Soc. Am. B **20**, 1769 (2003).
[33] A. P. Heberle, J. J. Baumberg, and K. Köhler, Phys. Rev. Lett. **75**, 2598 (1995).
[34] J. J. Baumberg, A. P. Heberle, K. Köhler, and K. Ploog, J. Opt. Soc. Am. B **13**, 1246 (1996).
[35] M. U. Wehner, J. Hetzler, and M. Wegener, Phys. Rev. B **55**, 4031 (1997).
[36] X. Marie, P. LeJeune, T. Amand, M. Brousseau, J. Barrau, M. Paillard, and R. Planel, Phys. Rev. Lett. **79**, 3222 (1997).
[37] N. H. Bonadeo, J. Erland, D. Gammon, D. Park, D. S. Katzer, and D. G. Steel, Science **1473**, 282 (1998).
[38] X. Marie, P. Renucci, S. Dubourg, T. Amand, P. LeJeune, J. Barrau, J. Bloch, and R. Planel, Phys. Rev. B **59**, R2494 (1999).
[39] Y.-S. Lee, T. B. Norris, A. Maslov, D. S. Citrin, J. Prineas, G. Khitrova, and H. M. Gibbs, Appl. Phys. Lett. **78**, 3941 (2001).
[40] J. Erland, V. G. Lyssenko, and J. M. Hvam, Phys. Rev. B **63**, 155317 (2001).
[41] A. Hache, Y. Kostoulas, R. Atanasov, J. L. P. Hughes, J. E. Sipe, and H. M. van Driel, Phys. Rev. Lett. **78**, 306 (1997).

[42] M. J. Stevens, A. L. Smirl, R. D. R. Bhat, A. Najmaie, J. E. Sipe, and H. M. van Driel, Phys. Rev. Lett. **90**, 136603 (2003).
[43] J. Hübner, W. W. Rühle, M. Klude, D. Hommel, R. D. R. Bhat, J. E. Sipe, and H. M. van Driel, Phys. Rev. Lett. **90**, 216601 (2003).
[44] X. Li, Y. Wu, D. Steel, D. Gammon, T. H. Stievater, D. S. Katzer, D. Park, C. Piermarocchi, and L. J. Sham, Science **301**, 809 (2003).
[45] V. M. Axt and A. Stahl, Z. Phys. B: Condens. Matter **93**, 195 (1994).
[46] V. M. Axt and S. Mukamel, Rev. Mod. Phys. **70**, 145 (1998).
[47] H. G. Breunig, T. Voss, I. Rückmann, and J. Gutowski, Phys. Rev. B **66**, 193302 (2002).
[48] T. Voss, H. G. Breunig, I. Rückmann, and J. Gutowski, Opt. Commun. **218**, 415 (2003).
[49] In the literature, t_{del} is often defined as positive for the direction $2k_i$-k_j if the pulse from direction k_j arrives at the sample first. For the present work we have deliberately chosen another definition to simplify the discussion because for the coherent-control experiments the same *sequence* of the excitation pulses—i.e., single pulse before or after the pulse pair—leads to comparable results for both FWM directions.
[50] W. Langbein and J. M. Hvam, Phys. Rev. B **61**, 1692 (2000).
[51] V. M. Axt and A. Stahl, Z. Phys. B: Condens. Matter **93**, 205 (1994).
[52] K. Victor, V. M. Axt, and A. Stahl, Phys. Rev. B **51**, 14164 (1995).
[53] N. H. Kwong, R. Takayama, I. Rumyantsev, M. Kuwata-Gonokami, and R. Binder, Phys. Rev. Lett. **87**, 027402 (2001).
[54] N. H. Kwong, R. Takayama, I. Rumyantsev, M. Kuwata-Gonokami, and R. Binder, Phys. Rev. B **64**, 045316 (2001).
[55] V. M. Axt, K. Victor, and T. Kuhn, Phys. Status Solidi B **206**, 189 (1998).
[56] S. Savasta, O. Di Stefano, and R. Girlanda, Phys. Rev. B **64**, 073306 (2001).
[57] S. Savasta, O. Di Stefano, and R. Girlanda, Phys. Rev. Lett. **90**, 096403 (2003).
[58] V. M. Axt, T. Kuhn, B. Haase, U. Neukirch, and J. Gutowski, Phys. Rev. Lett. **93**, 127402 (2004).
[59] E. J. Mayer *et al.*, Phys. Rev. B **51**, 10909 (1995).
[60] G. Finkelstein, S. Bar-Ad, O. Carmel, I. Bar-Joseph, and Y. Levinson, Phys. Rev. B **47**, 12964 (1993).
[61] H. P. Wagner, A. Schätz, W. Langbein, J. M. Hvam, and A. L. Smirl, Phys. Rev. B **60**, 4454 (1999).
[62] K. Victor, V. M. Axt, G. Bartels, A. Stahl, K. Bott, and P. Thomas, Z. Phys. B: Condens. Matter **99**, 197 (1996).
[63] One repeatedly encounters the technical problem that products of δ and step functions occur which are defined only as a limiting procedure starting from finite pulse durations. Here, we used the representation $\delta(t)=\lim_{\varepsilon\to 0^+}\theta(t)\theta(\varepsilon-t)/\varepsilon$ and took the limit explicitly at the end of the calculation.
[64] M. A. Bouchene, V. Blanchet, C. Nicole, N. Melikechi, B. Girard, H. Ruppe, S. Rutz, E. Schreiber, and L. Wöste, Eur. Phys. J. D **2**, 131 (1998).
[65] V. M. Axt, G. Bartels, B. Haase, J. Meinertz, U. Neukirch, and J. Gutowski, Phys. Status Solidi B **221**, 205 (2000).
[66] B. Haase, Opt. Lett. **24**, 543 (1999).
[67] Even for a fixed well width, experimental values for the biexction binding energy can vary by a few meV depending on details of the barrier material (Ref. 68). The modeling of these details is not the goal of the present paper. For our specific sample we can adjust the difference in the beating periods by using a scaling factor of 0.9.
[68] B. Haase, U. Neukirch, J. Gutowski, J. Nürnberger, W. Faschinger, M. Behringer, D. Hommel, V. M. Axt, G. Bartels, and A. Stahl, J. Cryst. Growth **214**, 856 (2000).